Check for updates

Modelling of *Escherichia coli* removal by a low-cost combined drinking water treatment system

Stephen Siwila and Isobel C. Brink

ABSTRACT

This work presents mathematical modelling of *Escherichia coli* (*E. coli*) removal by a multi-barrier point-of-use drinking water system. The modelled system is a combination of three treatment stages: filtration by geotextile fabric followed by filtration and disinfection by silver-coated ceramic granular media (SCCGM) then granular activated carbon (GAC) filtration. The presented models accounted for removal mechanisms by each treatment stage. *E. coli* was modelled as a microbial particle. *E. coli* inactivation by SCCGM was modelled using the Chick's, Chick-Watson, Collins-Selleck and complete mix system bacterial inactivation kinetic models, which were considered adequately representative for describing the removal. Geotextile removal was modelled using colloidal filtration theory (CFT) for hydrosol deposition in fibrous media. The filtration removal contributions by the SCCGM and GAC were modelled using CFT for removal of colloidal particles by granular media. The model results showed that inactivation by silver in the SCCGM was the main bacterial removal mechanism. Geotextile and GAC also depicted appreciable removals. The theoretical modelling approach used is important for design and optimization of the multi-barrier system and can support future research in terms of material combinations, system costs, etc. Collector diameter, particle size, filtration velocity and contact time were identified as critical parameters for *E. coli* removal efficiency.

Key words | CFT models, combined system, disinfection models, *E. coli* removal modelling, SCCGM, system optimization

Stephen Siwila (corresponding author)
Isobel C. Brink
Department of Civil Engineering,
Water Engineering Division,
Stellenbosch University,
Private Bag X1, Matieland 7602, Cape Town,
South Africa
E-mail: *ssiwilatabbie@yahoo.co.uk*

HIGHLIGHTS

- Demonstrates that suitable removal mechanisms can be applied integrally to model bacterial removal of a combined drinking water system.
- Modelling of combined point-of-use drinking water systems is generally a new concept.
- System modelled as a series of three compartments, effluent of one compartment was modelled as influent to the next.
- Was useful in predicting that the main bacterial removal mechanism was inactivation by silver in the SCCGM.
- Important for design and optimization of the modelled and similarly combined systems.

doi: 10.2166/ws.2020.084

Downloaded from http://iwaponline.com/ws/article-pdf/20/5/1757/728513/ws020051757.pdf
by STELLENBOSCH UNIVERSITY user

GRAPHICAL ABSTRACT

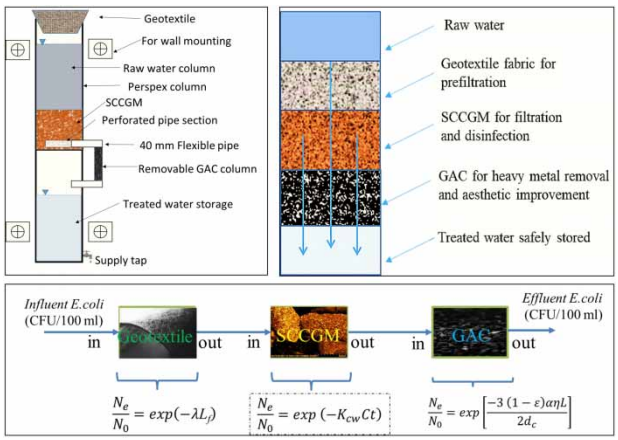

INTRODUCTION

Availability of safe drinking water is a major challenge in many rural and suburban areas of developing countries (Pandit & Kumar 2019; Treacy 2019). Globally, around 780 million rural and 136 million urban dwellers lack access to an improved drinking water supply (RWSN 2010). In sub-Saharan Africa, the discrepancy is even bigger with 272 million rural population lacking access to safe water, compared to 54 million in urban areas (RWSN 2010). Consumption of contaminated water results in waterborne disease outbreaks. Safe drinking water provision through point-of-use (PoU) water treatment is among the key measures required to prevent such outbreaks. While centralized piped water supply is the ideal solution for meeting drinking water needs in many communities worldwide (Lantagne & Yates 2018; Pandit & Kumar 2019), PoU water treatment has been shown by various authors (CAWST 2011; Kausley *et al.* 2018; Lantagne & Yates 2018; Pandit & Kumar 2019; Treacy 2019) to improve drinking water safety and reduce the burden of waterborne diseases. It is sometimes the only cost-effective option in many rural and suburban areas of developing countries. Although efforts to develop simple yet effective low-cost PoU technologies for rural and suburban areas have intensified globally (Treacy 2019), challenges still exist (Treacy 2019). Therefore, there is still need for development and/or optimization of more PoU techniques appropriate to poor communities. Mathematical modelling may assist in the design and optimization (costs, material combination, etc.) of various PoU systems and can support further research in terms of configuration, flow rate, media combination, and so on while also serving as a decision support tool.

Low-cost PoU water treatment technologies can be broadly classified into five groups (Lantagne & Yates 2018): (1) chemical disinfection (e.g. chlorine disinfection); (2) disinfection by heat (e.g. boiling), ultraviolet or solar radiation; (3) coagulation, flocculation, and sedimentation; (4) filtration (e.g. slow sand filtration); and (5) combined (multi-barrier) systems (CAWST 2011; Pandit & Kumar 2019). The priority of most PoU systems is to make water bacteriologically safe (CAWST 2017, 2011) and aesthetically acceptable (WHO 2017). Good aesthetic quality promotes health gains from drinking safe water (Lantagne & Yates 2018). Water of poor aesthetic quality, although safe, is often avoided (WHO 2017). Additionally, particles that contribute to poor aesthetic quality hinder bacterial inactivation (WHO 2017).

A thorough review of literature showed that modelling of PoU and similar systems for contaminant removal or system optimization has mainly been done on uncombined systems, for example: (i) intermittently operated slow sand

Downloaded from http://iwaponline.com/ws/article-pdf/20/5/1757/728513/ws020051757.pdf
by STELLENBOSCH UNIVERSITY user

filters (Fulazzaky *et al.* 2009; Jenkins *et al.* 2011), (ii) disinfection using chlorine (Lee & Nam 2002), (iii) disinfection by natural herbs (Somani & Ingole 2012), (iv) disinfection by silver or silver-coated materials (Chong *et al.* 2011; Rossainz-Castro *et al.* 2016; Singh *et al.* 2019), (v) granular activated carbon filtration (Hijnen *et al.* 2010), (vi) filtration by geotextile fabrics and other fibrous filter media (Choo & Tien 1991; Siwila & Brink 2018), and (vii) ultraviolet disinfection (Brownell *et al.* 2008), etc.

This paper presents modelling of *Escherichia coli* removal by a combined drinking water system developed by the authors (Siwila & Brink 2020) as a contribution to research and development on low-cost PoU drinking water treatment. The combined system consists of three treatment stages: pre-filtration by geotextile fabric followed by filtration and disinfection by SCCGM then GAC filtration (Siwila & Brink 2020). Each of these steps were modelled as a series of compartments by using specialized theoretical removal mechanisms for each barrier. *E. coli* was modelled as a microbial colloid or particle as proposed in literature (Tufenkji *et al.* 2003; Hijnen *et al.* 2010).

E. coli inactivation by SCCGM was modelled using Chicks, Chick-Watson, complete mix system and Collins-Selleck disinfection models (MWH 2012; Metcalf & Eddy 2014; Qasim & Zhu 2018), which were considered sufficiently representative to describe the removal. The Chick's and Chick-Watson models have been applied by various authors (Rossainz-Castro *et al.* 2016; Shimabuku *et al.* 2018; Singh *et al.* 2019) to model bacterial removal by silver and other metals. Additionally, Chick worked with silver nitrate among other disinfectants and *E. coli* among other organisms (MWH 2012). Geotextile removal was modelled using colloidal filtration theory (CFT) models for removal of hydrosols by fibrous media developed by Guzy *et al.* (1983) and Choo & Tien (1991) as presented by Tien (2012). The filtration removals by the SCCGM and GAC were modelled using the Yao CFT model for removal of colloidal particles from liquids by granular media developed by Yao *et al.* (1971) then refined by Rajagopalan & Tien (1976) (the RT model) and expanded further by Tufenkji & Elimelech (2004) (the TE model) (MWH 2012). The highlighted removal theories, governing equations and respective modelling procedure are explained in the methodology section of this paper.

Applied modelling of multi-barrier systems such as presented here can be helpful to system design and optimization (MWH 2012). This can help engineers understand the governing characteristics and contribution of each barrier to the effluent quality, subsequently enabling them to make informed decisions on the appropriate optimization measures. The importance of each treatment stage and associated removal mechanisms can be assessed as a function of system parameters (MWH 2012). This can allow engineers to vary design parameters until the desired system effectiveness and cost are achieved. For example, the modelling may assist in minimizing cost while ensuring the system is effective while deciding on which component needs more attention to increase removal efficiency of the water quality parameter of interest.

Since testing for every possible pathogen in water is difficult, time consuming, and expensive, indicator organisms such as *Escherichia coli* are often employed to assess bacteriological safety of drinking water (CAWST 2017). The presence of *E. coli* is definitive evidence of fecal contamination (Horan 2003; Brandt *et al.* 2017). Thus, if *E. coli* is detected in treated water, it indicates the presence of fecal matter and potentially pathogens (CAWST 2017). This signals potential malfunctioning in the responsible water treatment system posing a health risk requiring urgent action. In addition, *E. coli* has been indicated to be a better indicator for predicting diarrhoeal and gastrointestinal disease-causing pathogens than fecal coliforms particularly when detected in tropical drinking waters (Horan 2003; Brandt *et al.* 2017; Qasim & Zhu 2018). Therefore, bacterial removal by use of *E. coli* was chosen for modelling in this research. However, future research should expand to include the other pathogen classes (i.e. viruses, protozoa and helminths).

MATERIALS AND METHODS

The general experimental methodology aspects (study setting, design aspects, set up, sampling, testing methods, etc.) are presented in Siwila & Brink (2020). For instance, the measured *E. coli* log removal values (Table 4 and Figure 4) and contact time (Table 4) and resulting Ct values were calculated based on the work done in Siwila

Downloaded from http://iwaponline.com/ws/article-pdf/20/5/1757/728513/ws020051757.pdf
by STELLENBOSCH UNIVERSITY user

& Brink (2020). Furthermore, flow rate measurement, sample collection, contact time estimation, etc. as well as *E. coli* testing and enumeration procedures are given in Siwila & Brink (2020). The methodology for the present work primarily presents the mathematical modelling approach for prediction of *E. coli* removal by the modelled system. The schematic diagram of the combined system that is modelled is given in Figure 1. The system consisted of geotextile fabric for pre-filtration, SCCGM for filtration and disinfection, GAC filtration and a safe storage compartment for treated water. The key system parameters, particularly, those applied directly to the modelling in this paper are included in Table 1.

Sampling was done after at least 7.5 liters of water was passed through the system and at varied flow rates for the first 9 runs and at 2 L/h for the last 3 runs (Siwila & Brink 2020). The first four filtration runs were done at the maximum obtainable flow rate of 10 L/h (Table 4), while subsequent flow rates were varied from 8 L/h to 2 L/h (Table 4). Varying the flow rate was done to arrive at an optimal flow rate and produce varied contact time, and provide data for the modelling done here. Thus, flow rates were staggered from the highest obtainable to an optimal 2 L/h where 0 CFU/100 ml for *E. coli* and fecal coliform in the effluent (>99.99% removal) were consistently achieved.

E. coli removal performance modelling procedure

E. coli removal by the combined system was modelled as a series of three compartments. The models were coupled as depicted in Figure 2, whereby the effluent from the geotextile was modelled as the influent to the SCCGM and effluent from the SCCGM was modelled as influent to the GAC. Thus, the effluent of one compartment was modelled as influent to the next (Masters & Ela 2014). This modelling approach was derived from the works of (i) Metcalf & Eddy (2014), who modelled a number of wastewater reactors in series for pollutant removal, (ii) Rietveld (2019), who modelled a large-scale multi-barrier water treatment plant comprising ozone and sand filtration for *E. coli* reduction as units in series, as well as (iii) Masters & Ela (2014), who modelled a four-chamber tank for large scale drinking water disinfection as tanks in series.

E. coli removal was calculated using numerical models appropriate to each compartment. Input parameters (Table 1) used in the mathematical calculations were obtained using experimental data and from literature. The modelled removals were then calculated using Equation (1) adapted from de Moel *et al.* (2007) and Tien (2012) while log removal values (LRV) were obtained using Equation (2) adapted from MWH (2012). The total removal efficiency for each experimental run was calculated using Equation (3) (Tien 2012) and was then applied to the influent *E. coli* counts for each run. Computation and

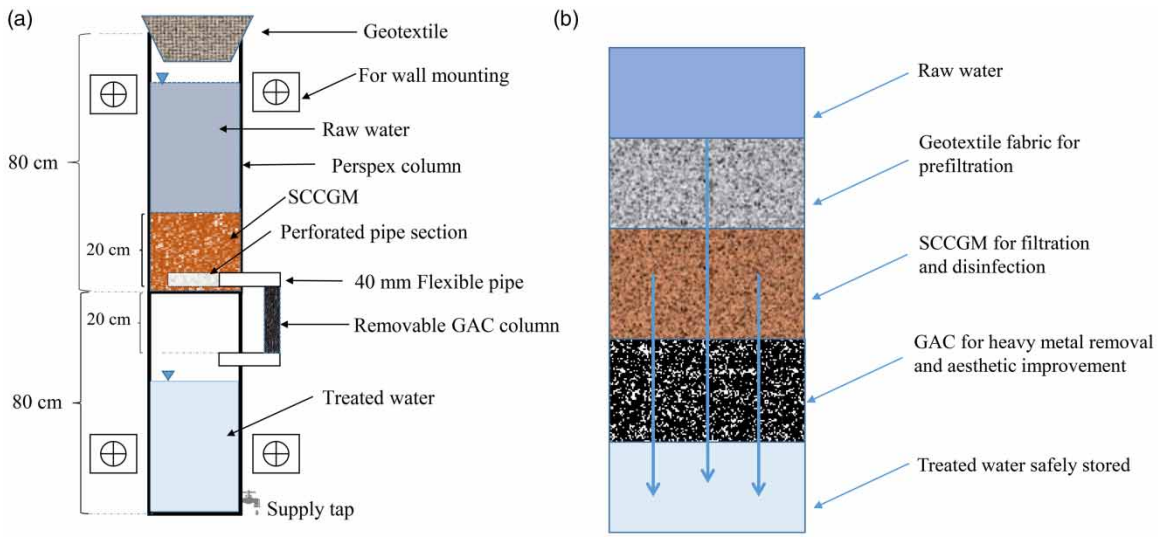

Figure 1 | Novel multi-barrier filter system, (a) designed system and (b) process schematic diagram (Siwila & Brink 2020).

Downloaded from http://iwaponline.com/ws/article-pdf/20/5/1757/728513/ws020051757.pdf
by STELLENBOSCH UNIVERSITY user

Table 1 | Key input parameter values used in the numerical computations

Parameter	Units	Value	Source of parameter and/or data used to calculate the parameter
Microbial particle (*E. coli*) size (d_p)	m	0.0000015	Medema *et al.* (1998); Qasim & Zhu (2018)
Diameter of the collector (d_c) for GAC	m	0.0006	Siwila & Brink (2020)
GAC media porosity (ε)	–	0.34	Siwila & Brink (2020)
Attachment efficiency (α) for GAC	–	0.57	Hijnen *et al.* (2010)
Absolute temperature (T) of water	K	298.15	Siwila & Brink (2020)
E. coli density (ρ_p)	kg/m^3	1,100	Bouwer & Rittmann (1992)
Acceleration due to gravity (g)	m/s^2	9.81	MWH (2012)
Density of water (ρ_w)	kg/m^3	997	Metcalf & Eddy (2014)
Dynamic viscosity (μ)	kg/m·s	0.00089	Metcalf & Eddy (2014)
Filtration rate (v_f) for GAC and SCCGM	m/h	0.34–1.72	Siwila & Brink (2020)
GAC bed depth (L)	m	0.2	Siwila & Brink (2020)
Hamaker constant (H_a) for *E. coli* PVC water interface	$kg{\cdot}m^2/s^2$	9.72E-20	Rijnaarts *et al.* (1995)
Boltzmann constant (k_B)	$kg{\cdot}m^2/s^2{\cdot}K$	1.381E-23	MWH (2012); Tobiason *et al.* (2011)
Empty bed contact time (EBCT)	h	0.12–0.58	Siwila & Brink (2020)
Chick's model inactivation constant, k_o	min^{-1}	0.21	Siwila & Brink (2020)
Chick-Watson coefficient of specific lethality, K_{cw}	L/mg·min	0.103	TAM Ceramics (2019)
Range of Ct values for Chick-Watson model	mg·min/L	13.9–69.7	Siwila & Brink (2020)
Geotextile fabric porosity (ε)	–	0.75	Kaytech Engineering (2018)
Geotextile single fiber diameter (d_f)	μm	25	Kaytech Engineering (2018)
Geotextile total thickness (h)	mm	36	Siwila & Brink (2020)
Geotextile solidity (Φ)	–	0.25	Siwila & Brink (2020)
Filtration rate (v_f) for the geotextile	m/s	0.0098	Siwila & Brink (2018)
Hamaker constant (H_a) for *E. coli* geotextile water interface	$kg{\cdot}m^2/s^2$	6.48E-20	Rijnaarts *et al.* (1995)
Diameter of the collector (d_c) for SCCGM	m	0.0005	TAM Ceramics (2019)
SCCGM bed depth (L)	m	0.2	Siwila & Brink 2020
SCCGM porosity (ε)	–	0.30	TAM Ceramics (2019)
Hamaker constant (H_a) for *E. coli* SCCGM water interface	$kg{\cdot}m^2/s^2$	8.10E-20	Rijnaarts *et al.* (1995)
Attachment efficiency (α) for SCCGM	–	0.10	Tufenkji *et al.* (2003)

integration of removal efficiencies by each stage (Figure 2 and Table 3) and respective removal mechanisms was done in Microsoft Excel 2016. Statistical analysis was done using Tool Pak VBA a Microsoft Excel 2016 add-in.

$$\text{Removal}_{predicted} = \left(1 - \frac{N_e}{N_o}\right) \quad (1)$$

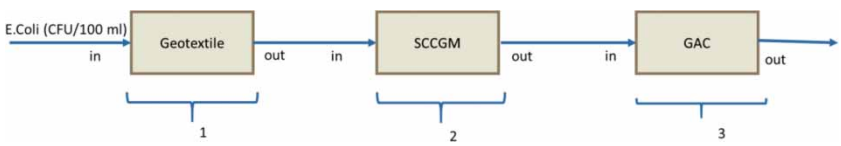

Figure 2 | Definition sketch for modelling the multi-barrier system's *E. coli* removal using compartments in series.

Downloaded from http://iwaponline.com/ws/article-pdf/20/5/1757/728513/ws020051757.pdf
by STELLENBOSCH UNIVERSITY user

where: N_o = Influent *E. coli* count [CFU/100 ml]; N_e = Effluent *E. coli* count [CFU/100 ml];

$\text{Removal}_{predicted}$ = Predicted removal fraction

$$LRV_{predicted} = -log_{10}\left(\frac{N_e}{N_o}\right) \quad (2)$$

where: $LRV_{predicted}$ = Predicted log removal value

$$\eta_{total\ efficiency} = 1 - [(1 - \eta_{geotextile})(1 - \eta_{SCCGM})(1 - \eta_{GAC})] \quad (3)$$

where: $\eta_{geotextile}$ = geotextile removal efficiency; η_{SCCGM} = SCCGM removal efficiency; η_{GAC} = GAC removal efficiency.

Remembering that the length of the filter bed and the residence time play key roles in determining bacterial removals, contact time between *E. coli* and silver was estimated using Equation (4), adapted from Metcalf & Eddy (2014), for each run and flow rate

$$EBCT = \frac{V_{media}}{Q_v} = \frac{V_{media}}{v.A} = \frac{h.A}{v.A} = \frac{h}{v} \quad (4)$$

where: EBCT = empty bed contact time (h); Q_v = flow rate (m^3/h); A = cross sectional area of GAC or SCCGM filter bed (m^2) of diameter d (m) $\left(A = \frac{\pi d^2}{4}\right)$; V_{media} = column volume occupied by GAC or SCCGM (m^3); v = filtration velocity (m/h); h = height of GAC or SCCGM bed (m).

A total of eight combined mathematical models (see Table 3) were tested using combinations of disinfection and filtration modelling approaches as given below. The respective disinfection and filtration modelling approaches alongside the various *E. coli* removal mechanisms and parameter equations are explained below. Thereafter, the eight combined models as were used in the numerical calculations of this study are summarized in Table 3 and the associated text just above Table 3.

Modelling *E. coli* removal by the SCCGM

E. coli removal by SCCGM was first modelled using disinfection kinetics in the first four combined models (see Table 3). The removal was thereby modelled as being only due to bacterial inactivation by the silver coating of the media. The inactivation by silver was modelled using Chick's, Collins-Selleck, complete-mix system (CMS) model and the Chick-Watson bacterial inactivation models (de Moel *et al.* 2007; Metcalf & Eddy 2014) explained below. Thereafter, *E. coli* removal contribution by SCCGM filtration (Table 3) was included in the last four combined models using the colloidal filtration theory (CFT) numerical modelling procedure explained under *E. coli* removal by GAC filtration, but using appropriate SCCGM characteristics.

Chick's and Plug flow model

Assuming that for any length, dx, and throughout the corresponding cross section, (i) mixing of the microbial particles is ideal (Figure 3), (ii) flow rate is constant, and (iii) no storage exists in the SCCGM filter bed, mass balance was done as follows (de Moel *et al.* 2007):

Inlet = outlet + decay

$$QN = Q(N + dN) + k_o NA dx \quad (5)$$

where: Q = flow rate, N = *E. coli* count (CFU/100 ml), dx = length; k_o = mortality or inactivation rate (CFU inactivated/min), A = cross-sectional area

Simplifying Equation (5) gives Equation (6):

$$\frac{1}{N}dN = -k_o \frac{A}{Q}dx \quad (6)$$

Applying the following boundary conditions to the SCCGM filter bed: (i) at x = 0; $N = N_o$, and (ii) at x = L;

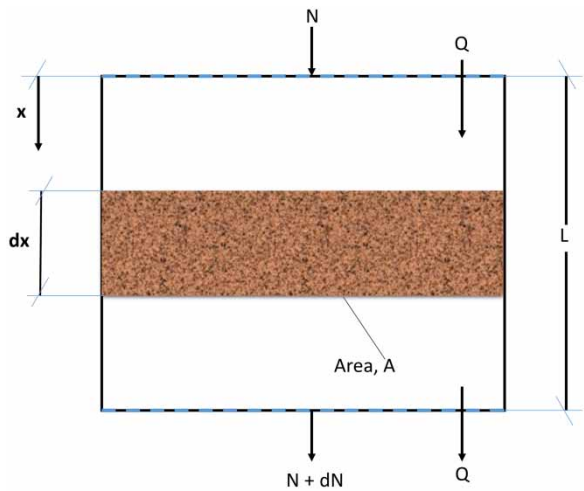

Figure 3 | Schematic element for the plug flow model.

Downloaded from http://iwaponline.com/ws/article-pdf/20/5/1757/728513/ws020051757.pdf
by STELLENBOSCH UNIVERSITY user

$N = N_e$, and remembering that $\frac{AL}{Q} = \frac{V}{Q} = t$; yields Equation (7) (de Moel *et al.* 2007):

$$\Rightarrow \frac{N_e}{N_o} = exp\ (-k_o t) \tag{7}$$

where: N_o = Influent *E. coli* count [CFU/100 ml]; N_e = Effluent *E. coli* count [CFU/100 ml]; $\left(\frac{N_e}{N_o}\right)$ = fraction of influent *E. coli* [CFU/100 ml] remaining in the effluent, t = time (in this study, $t \approx$ EBCT (de Moel *et al.* 2007)). k_o ($CFU\ inactivated/min$) was estimated by plotting $-\ln\left(\frac{N_e}{N_o}\right)$ versus contact time, where k_o is the gradient of the best fit line (Metcalf & Eddy 2014).

Since the form of Equation (7) is exactly like the Chick's model (Chick 1908; MWH 2012; Metcalf & Eddy 2014; Qasim & Zhu 2018) for disinfection, it was handled as such to simplify the theoretical approach. The Chick's model (Equation (7)) and Chick-Watson model (Equation (11)) were also used by Rossainz-Castro *et al.* (2016) to model *E. coli* and *Candida albicans* inactivation by silver and copper-coated granular zeolite, by Singh *et al.* (2019) to model *E. coli* inactivation by silver and other metals as well as by Somani & Ingole (2012) for kinetic modelling of water disinfection by natural herbs.

Complete mixing system (CMS) model

The SCCGM bed was modelled as having a volume V (m^3) fed by a flow rate Q and an *E. coli* count N_o and with effluent *E. coli* count of N_e and flow rate Q same as the influent flow rate. Steady state mass balance for the filter bed was as follows (de Moel *et al.* 2007; Masters & Ela 2014):

Inlet = outlet + decay

$$QN_o = QN_e + k_o V N_e$$

$$\Rightarrow 0 = QN_o - QN_e - k_o V N_e \tag{8}$$

Solving for N_e and remembering that $t = \frac{V}{Q}$, then rearranging gives Equation (9)

$$\Rightarrow N_e = \frac{QN_0}{Q + Vk_o}$$

$$\Rightarrow \frac{N_e}{N_0} = \frac{1}{1 + k_0 t} \tag{9}$$

where: N_o = Influent *E. coli* count [CFU/100 ml]; N_e = Effluent *E. coli* count [CFU/100 ml]; k_o = mortality or inactivation rate; t = contact time (in this study, t ≈ EBCT (de Moel *et al.* 2007)).

The Collins-Selleck model

The Collins-Selleck model Equation (10) (Metcalf & Eddy 2014) was developed by Collins for chemical disinfection of coliform bacteria in domestic wastewater (MWH 2012). The model has overtime been proven valuable for modelling bacterial inactivation by various alternative disinfectants as well (MWH 2012).

$$\frac{N_e}{N_0} = \frac{1}{(1 + 0.23Ct)^3} \tag{10}$$

where: C = concentration of disinfectant, mg/L; t = contact time (in this study, T ≈ EBCT (de Moel *et al.* 2007)).

The Chick-Watson model

The Chick-Watson model Equation (11) is a refined version of the Chick's model and emphasizes that time required to achieve a certain inactivation level is related to the disinfectant concentration (MWH 2012; Metcalf & Eddy 2014).

$$\frac{N_e}{N_0} = exp\ (-K_{cw} Ct) \tag{11}$$

where: N_o = Influent *E. coli* count [CFU/100 ml]; N_e = Effluent *E. coli* count [CFU/100 ml]; C = concentration of disinfectant [mg/L]; t = contact time [s]; Kcw = specific lethality [L/(mg·min)] and was estimated by plotting *-ln(Ne/No)* versus *Ct* (concentration x contact time) and obtaining the slope for the best fit line (MWH 2012; Metcalf & Eddy 2014; Qasim & Zhu 2018) using experimental data; *Ct* was calculated by multiplying C by t (MWH 2012; Metcalf & Eddy 2014).

Downloaded from http://iwaponline.com/ws/article-pdf/20/5/1757/728513/ws020051757.pdf
by STELLENBOSCH UNIVERSITY user

E. coli removal modelling by the GAC filtration

The removal of *E. coli* as microbial particles by GAC was modelled using the Yao CFT approach (Yao *et al.* 1971; MWH 2012) by relating the *E. coli* removal performance of the GAC column of depth L to the SCE of GAC (Equation (12)). Doing a mass balance on a small differential element and integrating over the entire depth Equation (12) gives Equation (13), which is the classical Yao CFT model (Yao *et al.* 1971; Tobiason *et al.* 2011; MWH 2012). Particle removal from water is modelled based on the single collector efficiency (SCE) model (Equation (14)). The fraction of particles that actually get captured by a single collector is a product of the SCE (η) and the attachment efficiency (α) (Equations (12) and (13)).

$$\frac{\partial \mathrm{N}}{\partial \mathrm{L}} = -\lambda N = -\left(\frac{3}{2}\frac{(1-\varepsilon)}{d_c}\alpha\eta\right)\mathrm{N} \tag{12}$$

where: λ = filter coefficient, ε = porosity of GAC, L = column depth (m), α = attachment efficiency, which reflects the chemistry of the system, η = SCE, d_c = diameter of collector (m), N = concentration of microbial particles (*E. coli*).

$$\frac{N_e}{N_0} = \exp\left[\frac{-3\ (1-\varepsilon)\alpha\eta\mathrm{L}}{2d_c}\right] \tag{13}$$

where: N_e = effluent concentration of *E. coli* (CFU/100 ml); N_o = influent concentration of *E. coli* (CFU/100 ml);

The η and α respectively give the fractions of *E. coli* contacting and being retained by the GAC grains as defined by Equations (14) and (15). SCE (η) was computed using the optimized SCE model (Equation (14)) presented by Tufenkji & Elimelech (2004), which is a semi-empirical expression that was derived using results of numerical simulations (MWH 2012). It is an expansion on Rajagopalan and Tien's SCE model and fully integrates hydrodynamic and van der Waal forces interactions into all particle removal mechanisms (MWH 2012). The removal efficiencies by each mechanism (interception, sedimentation and diffusion) are assumed as additive and are accounted for in the SCE. The parameters in the TE model are defined in Table 2, while the summary of the input values for the present study are given in Table 1.

$$\eta\,(SCE) = \frac{E.coli\ bacteria\ contacting\ the\ GAC\ collector}{E.coli\ bacteria\ approaching\ the\ GAC\ collector} = \eta_D + \eta_I + \eta_G$$

$$= 2.4A_s^{\left(\frac{1}{3}\right)}N_R^{-0.081}N_{pe}^{-0.715}N_{vdw}^{0.052} + 0.55A_sN_R^{1.675}N_A^{0.125} + 0.22N_R^{-0.24}N_G^{1.11}N_{vdw}^{0.053} \tag{14}$$

where: η_D = transport due to diffusion, η_I = transport due to interception, η_G = transport due to gravity

$$\alpha\ (attachment\ efficiency) = \frac{E.coli\ bacteria\ sticking\ to\ the\ collector}{E.coli\ bacteria\ contacting\ the\ collector} \tag{15}$$

Theoretically α ranges between 0 and 1 from poor to optimal sticking conditions respectively (Tufenkji & Elimelech 2004; Tobiason *et al.* 2011).

E. coli removal modelling by the geotextile fabric

The prediction of *E. coli* removal as a microbial particle by the geotextile was modelled using CFT filter coefficients for hydrosol deposition in fibrous media (Tien 2012). The correlations were originally derived by Guzy *et al.* (1983) and Choo & Tien (1991), who assumed that removal of hydrosols in fibrous media is due to combined effects of gravitational settling, interception and the London-van der Waals force (Tien 2012). Guzy *et al.* (1983) and Choo & Tien (1991) did trajectory analysis using various cylinder-in-cell models to obtain filter coefficient correlations under conditions of favorable surface interactions (Tien 2012). They considered molecular dispersion, electro kinetic and hydrodynamic forces on the hydrosol using Swarm theory for flow through a system of fibers (Guzy *et al.* 1983). Using results from their application of Kuwabara's cylinder-in-cell model, Choo & Tien (1991) derived the correlation applied in the present study as given by

Downloaded from http://iwaponline.com/ws/article-pdf/20/5/1757/728513/ws020051757.pdf
by STELLENBOSCH UNIVERSITY user

Table 2 | Definitions of the TE model SCE equations and parameters adapted from MWH (2012) and Tobiason *et al.* (2011)

Parameter	Definition equation	Parameter	Definition
N_R (relative size group, dimensionless)	$N_R = \frac{d_p}{d_c}$	d_p	Particle diameter (m)
N_G (gravity number, dimensionless)	$N_G = \frac{V_S}{V_F} = \frac{g(\rho_p - \rho_w)(d_p)^2}{18\mu V_F}$	d_c	Collector diameter (m)
N_A (attraction number, dimensionless)	$N_A = \frac{N_{vdw}}{N_R N_{Pe}} = \frac{H_a}{3\pi\mu(d_p)^2 V_F}$	k_B	Boltzmann's constant, $(1.381 \times 10^{-23}$ J/K)
N_{vdw} (van der Waals number, dimensionless)	$N_{vdw} = \frac{H_a}{k_B T}$	ε	Filter media porosity, dimensionless
N_{pe} (Peclet number, dimensionless)	$N_{pe} = \frac{V_F d_c}{D_L} = \frac{3\pi\mu d_p d_c V_F}{k_B T}$	g	Gravitational acceleration (m/s^2)
A_s (porosity dependent function, dimensionless)	$A_s = \frac{2(1-\gamma^5)}{2-3\gamma+3\gamma^5-2\gamma^6}$	H_a	Hamaker constant (J)
D_L (diffusion coefficient, m^2/s)	$D_L = \frac{k_B T}{3\pi\mu d_p}$	T	Absolute temperature, K (273 + ° C)
γ (porosity coefficient, dimensionless)	$\gamma = (1-\varepsilon)^{(\frac{1}{3})}$	V_F	Filtration rate (m/s)
		ρ_p	*E. coli* (particle) density, (kg/m^3)
V_s (Stokes' settling velocity, m/s)	$V_s = \frac{g(\rho_p - \rho_w)(d_p)^2}{18\mu}$	μ	Absolute viscosity of water (kg/m-s)
		ρ_w	Density of water (kg/m^3)

Equation (16) (Tien 2012).

$$\lambda_1 = \left(\frac{6}{\pi}\right)\left(\frac{1-\varepsilon}{d_f}\right)A_s\,[0.216 \text{ x } 10^{-0.41\varepsilon}N_R^{1.55}N_{LO}^{0.1542} + 2.99\times10^{-4}\times10^{3\varepsilon}N_G^{1.1}N_R^{-0.3}] \quad (16)$$

For $10^{-3} < N_R < 10^{-1}$;
$10^{-4} < N_G < 10^{-1}$;
$10^{-8} < N_{LO} < 10^{-3}$;
$0.01 < \Phi < 0.65$;

where: λ_1 = filter coefficient, ε = porosity, N_R = interception parameter defined by Equation (17a) N_G = dimensionless gravitational parameter defined by Equation (17b); N_{LO} = London–van der Waals force parameter defined by Equation (17c); A_s = a hydrodynamic parameter for the Kuwabara cylinder-in-cell model defined by Equation (18a); Φ = solidity (packing density) = 1-ε, ε = geotextile porosity:

$$N_R = \frac{d_p}{d_f}; \quad (17a)$$

$$N_G = \frac{2g(\rho_p - \rho_w)a_p^2}{9\mu u_s}; \quad (17b)$$

$$N_{LO} = \frac{H_a}{9\pi\mu a_p^2 u_s} \quad (17c)$$

where: d_p = particle diameter (m), d_f = fiber diameter (m); μ = absolute viscosity of water (kg/m-s), u_s = filtration velocity (m/s); a_p = particle radius (m); ρ_p = particle density (kg/m^3), ρ_w = density of water (kg/m^3), H_a = Hamaker constant (J).

$$A_s = \frac{\left(\frac{2}{3}\right)(4C_1 + C_4)}{C_1\left(\left(\frac{1}{\Phi}\right) - 2 + \Phi\right) + \left(\frac{C_4}{2}\right)(\Phi - 1 - \ln\Phi)} \quad (18a)$$

$$C_1 = -\Phi\frac{C_4}{4} \quad (18b)$$

$$C_2 = -C_1 - C_3 \quad (18c)$$

$$C_3 = C_1 + \left(\frac{C_4}{2}\right) \quad (18d)$$

Downloaded from http://iwaponline.com/ws/article-pdf/20/5/1757/728513/ws020051757.pdf
by STELLENBOSCH UNIVERSITY user

$$C_4 = \frac{-4}{2\ln\Phi + 3 - 4\Phi + \Phi^2} \tag{18e}$$

$$\Phi = 1 - \varepsilon \tag{18f}$$

where: Φ = solidity (packing density) (m^3/m^3), ε = porosity.

To cater for the SFCE by Brownian diffusion, which is not accounted for in Equation (16), the filter coefficient accounting for Brownian diffusion (λ_{bm}) was calculated by Equation (19a) (Tien 2012) and was then added to λ_1 (Equation 20), assuming additivity (Tien 2012). Equation (19a) was established by Choo & Tien (1991) to account for hydrosol deposition by Brownian motion based on results of the convective diffusion equation solutions.

$$\lambda_{bm} = \left(\frac{9.2}{\pi}\right)(C_1 + C_3)\left(\frac{1}{3}\right)\left[\frac{(1-\varepsilon)}{d_f}\right]N_{pe}^{\left(\frac{-2}{3}\right)} \tag{19a}$$

$$N_{pe} = \frac{d_f u_s}{D_{BM}} \tag{19b}$$

$$D_{BM} = \frac{c_s K_B T}{3\pi\mu d_p} \tag{19c}$$

$$c_s = 1 + \frac{\ell}{a_p}\left[1.23 + 0.41exp\left(\frac{-0.88a_p}{\ell}\right)\right] \tag{19d}$$

$$\ell = \frac{\mu}{\sqrt{\frac{(2\rho_w P)}{\pi}}} \tag{19e}$$

where: N_{pe} = Peclet number, dimensionless; D_{BM} = Brownian diffusivity (m^2/s); ε = porosity c_s = Cunningham correction factor, K_B = Boltzmann constant (1.381×10^{-23} J/K), d_f = fiber diameter (m); μ = absolute viscosity of water (kg/m-s), u_s = filtration velocity (m/s); d_p = particle diameter (m), a_p = particle radius (m); ρ_w = density of water (kg/m^3); P = pressure (pa) assumed equal to atmospheric pressure (Tien (2012); T = temperature (K); C_1 and C_3 are as defined in Equation (18) above; ℓ = mean free path of water molecules (m).

Adding λ_1 and λ_{bm}, we obtain a geotextile filter coefficient (λ) that was used in Equation (23):

$$\lambda = \lambda_1 + \lambda_{bm} \tag{20}$$

Assuming further that the geotextile filter has the same porosity and uniform collector size distribution throughout its depth, the filter coefficient (λ) is defined in Equation (21) (Wakeman & Tarleton 2005):

$$\lambda = -\left(\frac{\delta_N}{N}\right)\left(\frac{1}{\delta L}\right) \tag{21}$$

where: $-\delta_N$ is the reduction of the concentration of *E. coli* as microbial particles passing through a layer of thickness δL. Rearranging the above equation yields Equation (22) (Wakeman & Tarleton 2005; MWH 2012).

$$-\frac{dN}{dL} = \lambda N \tag{22}$$

Representing the influent concentration of the microbial particles by N_0 and integrating Equation (22) with $L = 0$ (as initial conditions) at filter inlet, we obtained Equation (23) which was then used to estimate the fraction of microbial particle concentration remaining in the effluent.

$$\frac{N_e}{N_0} = \exp(-\lambda L) \tag{23}$$

where: N_e = effluent concentration of *E. coli* (CFU/100 ml); N_o = influent concentration of *E. coli* (CFU/100 ml); L = fibrous filter thickness, L_f (m).

Definitions of the combined system mathematical models

Overall, eight combined mathematical models as defined below and summarized in Table 3 were used in the numerical calculations of the present study. It is worth noting here that most of the model equations used are associated with the various removal mechanisms and parameter equations explained above.

Model 1 refers to the modelled combined removals, starting with geotextile filtration governed by Equation (23) coupled to SCCGM disinfection removals modelled by Chick's model (Equation (7)) followed by GAC filtration removals modelled by Equation (13). Model 2 refers to the modelled combined removals starting with geotextile

Downloaded from http://iwaponline.com/ws/article-pdf/20/5/1757/728513/ws020051757.pdf
by STELLENBOSCH UNIVERSITY user

filtration governed by Equation (23) coupled to SCCGM disinfection removals modelled by the complete mixing system model (Equation (9)) followed by GAC filtration removals modelled by Equation (13). Model 3 refers to the modelled combined removals starting with geotextile filtration governed by Equation (23) coupled to SCCGM disinfection removals modelled by the Collins-Selleck model (Equation 10) followed by GAC filtration removals modelled by Equation (13). Model 4 refers to the modelled combined removals starting with geotextile filtration governed by Equation (23) coupled to SCCGM disinfection removals modelled by Chick-Watson model (Equation 11) followed by GAC filtration removals modelled by Equation (13). Model 5 refers to the modelled combined removals of Model 1 plus SCCGM filtration contribution modelled by Equation (13). Model 6 refers to the modelled combined removals of Model 2 plus SCCGM filtration contribution modelled by Equation (13). Model 7 refers to the modelled combined removals of Model 3 plus SCCGM filtration contribution modelled by Equation (13). Model 8 refers to the modelled combined removals of Model 4 plus SCCGM filtration contribution modelled by Equation (13). Model calculations for each run began with *E. coli* counts in the influent then integrated removal efficiencies (Equation (3)) by each stage (Figure 2 and Table 3) were applied successively to the influent counts to get effluent *E. coli* counts and respective LRVs (Table 4).

Model performance assessment

The *E. coli* removal performance of each model was assessed using the following statistical techniques (Krause *et al.* 2005; Gikas & Tsihrintzis 2012; Chen & Liu 2015):

$$R^2 = 1 - \frac{SSE}{SST} = \left(\frac{\sum_{i=1}^{N} (O_i - O_{mean})(P_i - P_{mean})}{\sqrt{\sum_{i=1}^{N} (O_i - O_{mean})^2} \sqrt{\sum_{i=1}^{N} (P_i - P_{mean})^2} } \right)^2 \quad (24)$$

where: R^2 = coefficient of determination; SSE = sum of squared errors; SST = total sum of squares. P_i = model predicted value; O_i = observed value. P_{mean} = mean of predicted values; O_{mean} = mean of observed values. R^2 values range between 0.0 and 1.0. The ideal value of R^2 is 1.0, which signifies a perfect match between the predicted and measured values, while R^2 values larger than 0.5 are generally considered acceptable and indicate an acceptable fit. An R^2 value of 0.0 indicates there is no correlation between predicted and measured values.

$$RMSE = \sqrt{\frac{\sum_{i=1}^{N} (P_i - O_i)^2}{N}} \quad (25)$$

Table 3 | Summary of the *E. coli* removal prediction combined mathematical models

	Model 1	Model 2	Model 3	Model 4	Model 5	Model 6	Model 7	Model 8
E.coli counts	Influent	Influent	Influent	Influent	Influent	Influent	Influent	Influent
	↓	↓	↓	↓	↓	↓	↓	↓
Geotextile E.coli removal governed by:	Equation 23	Equation 23	Equation 23	Equation 23	Equation 23	Equation 23	Equation 23	Equation 23
SCCGM E.coli removal governed by:	Equation 7	Equation 9	Equation 10	Equation 11	Equation 7 plus, Equation 13	Equation 9 plus, Equation 13	Equation 10 plus, Equation 13	Equation 11 plus, Equation 13
GAC E.coli removal governed by:	Equation 13	Equation 13	Equation 13	Equation 13	Equation 13	Equation 13	Equation 13	Equation 13
	↓	↓	↓	↓	↓	↓	↓	↓
E.coli counts	Effluent	Effluent	Effluent	Effluent	Effluent	Effluent	Effluent	Effluent

Downloaded from http://iwaponline.com/ws/article-pdf/20/5/1757/728513/ws020051757.pdf
by STELLENBOSCH UNIVERSITY user

Table 4 | Measured and predicted *E. coli* log removal values for each run number

Run number	Flow rate (L/h)	Estimated contact time (h)	Chick-Watson model Ct values (mg·min/L)	Measured LRVs	Predicted LRVs							
					Model 1	Model 2	Model 3	Model 4	Model 5	Model 6	Model 7	Model 8
1	10	0.12	13.9	2.57	1.21	0.97	2.46	1.21	1.26	1.02	2.51	1.26
2	10	0.12	13.9	1.90	1.21	0.97	2.46	1.21	1.26	1.02	2.51	1.26
3	10	0.12	13.9	1.95	1.21	0.97	2.46	1.21	1.26	1.02	2.51	1.26
4	10	0.12	13.9	2.94	1.21	0.97	2.46	1.21	1.26	1.02	2.51	1.26
5	8	0.15	17.4	1.94	1.38	1.05	2.70	1.39	1.44	1.11	2.76	1.44
6	8	0.15	17.4	2.01	1.38	1.05	2.70	1.39	1.44	1.11	2.76	1.44
7	7	0.17	19.9	2.48	1.51	1.10	2.86	1.51	1.57	1.16	2.92	1.57
8	5	0.23	27.9	2.62	1.90	1.24	3.27	1.91	1.97	1.31	3.33	1.97
9	3	0.39	46.5	4.00	2.82	1.50	3.94	2.82	2.91	1.59	4.03	2.91
10	2	0.58	69.7	4.00	3.95	1.74	4.52	3.95	4.07	1.86	4.64	4.07
11	2	0.58	69.7	4.00	3.95	1.74	4.52	3.95	4.07	1.86	4.64	4.07
12	2	0.58	69.7	4.00	3.95	1.74	4.52	3.95	4.07	1.86	4.64	4.07

where: $RMSE$ = root mean squared error; N = total number of observations; P_i = model predicted value; O_i = observed value. The smaller the $RMSE$, the better the model predictions.

$$NOF = \frac{RMSE}{O_{mean}} \tag{26}$$

where: NOF = normalized objective function, and O_{mean} = mean of observed values. The optimal value of NOF is 0.0. However, the model is acceptable if NOF values range between 0.0 and 1.0. The smaller the NOF, the better the model predictions.

$$PBIAS = \left[\frac{\sum_{i=1}^{N}(O_i - P_i)*(100)}{\sum_{i=1}^{N}(O_i)}\right] \tag{27}$$

where: $PBIAS$ = Percent bias, and measures the average deviation between predicted and observed values expressed as a percentage; P_i = model predicted value; O_i = observed value. The ideal value of $PBIAS$ is 0.0, with smaller absolute values signifying more accurate predictions. Positive values signify model underestimation bias, while negative values indicate model overestimation bias.

Sensitivity analysis

Sensitivity analysis was carried to test (i) the effect of neglecting the filtration removal component by the SCCGM to the models, (ii) the effect of modelling *E. coli* removal by disinfection alone, and (iii) the sensitivity of contact time, filtration rate, collector diameter and microbial particle (*E. coli*) size to the models. Condition (i) was assessed by essentially comparing the predicted *E. coli* removals by models 1–4 with the corresponding removals by models 5–8 (Figure 4), while conditions (ii) and (iii) were tested using models 3 and 8 to test the sensitivity of simulated *E. coli* removal to each condition or parameter (Figures 5 and 6). The results of the sensitivity analysis are given and explained below under results and discussion.

RESULTS AND DISCUSSION

Comparison of measured and predicted effluent *E. coli* removals

Predicted *E. coli* removals were calculated using the coupled models presented above, which are based on the removal mechanisms elaborated on earlier. Figure 4 gives

Downloaded from http://iwaponline.com/ws/article-pdf/20/5/1757/728513/ws020051757.pdf
by STELLENBOSCH UNIVERSITY user

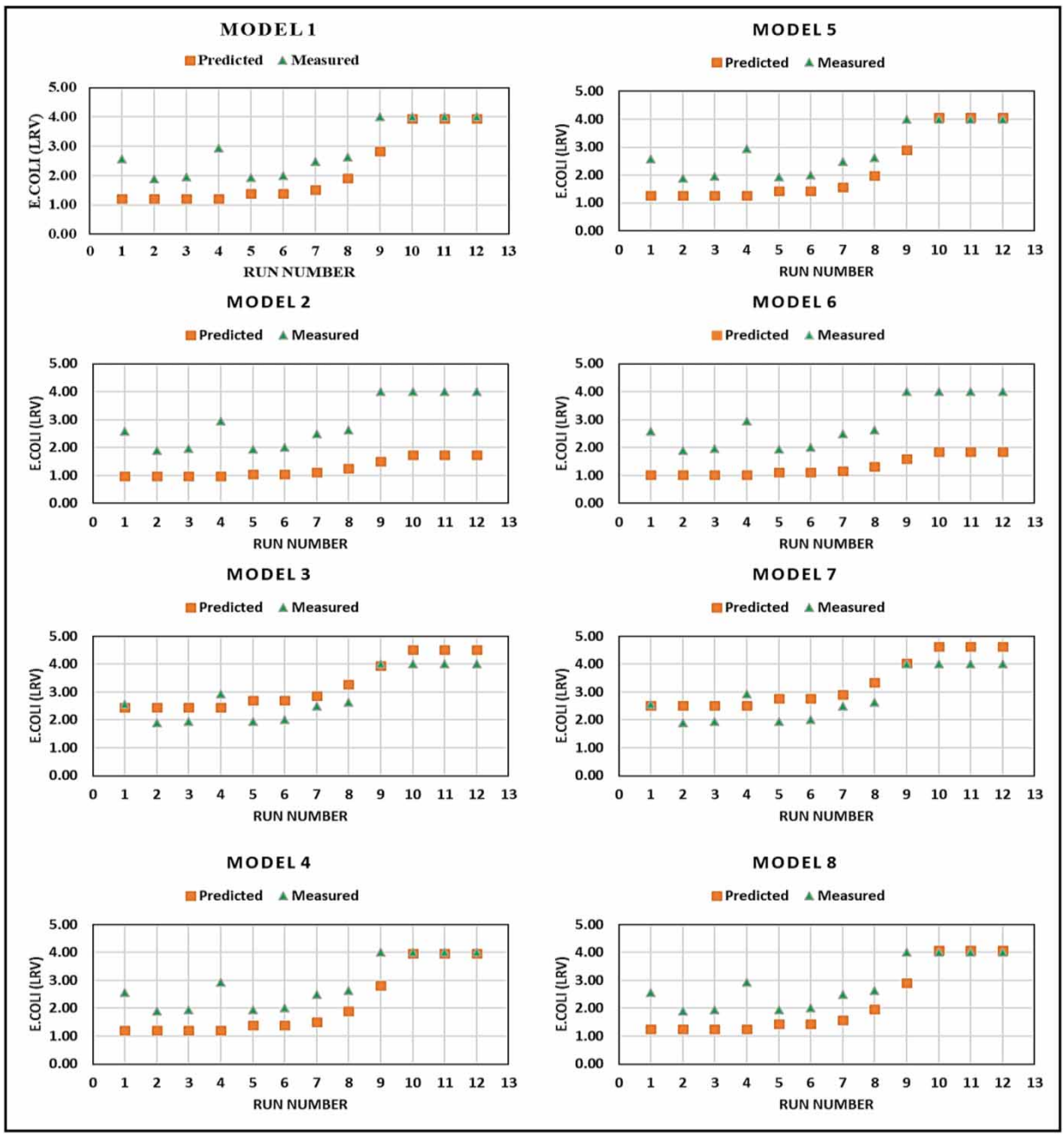

Figure 4 | Graphical visualization of predicted and measured *E. coli* log removal values.

comparative plots of theoretically predicted and measured *E. coli* Log Removal Values (LRVs) for each run and model respectively. The results (Figure 4 and Tables 4 and 5) show that the coupled models – except for models 2 and 6 – reasonably described the combined *E. coli* removals by the multi-barrier system. Although models 1, 4, 5, and 8 gave slight underestimations for runs with lower contact time, their predictions were considered satisfactory as also shown by the model performance criteria in Table 5. Models 3 and 7 gave the closest predictions of *E. coli* removal values with respect to the measured values, but generally overestimated the LRVs. The appreciable performance by models 1, 3, 4, 5, 7 and 8 signifies they simulated the combined physical and chemical *E. coli*

Downloaded from http://iwaponline.com/ws/article-pdf/20/5/1757/728513/ws020051757.pdf
by STELLENBOSCH UNIVERSITY user

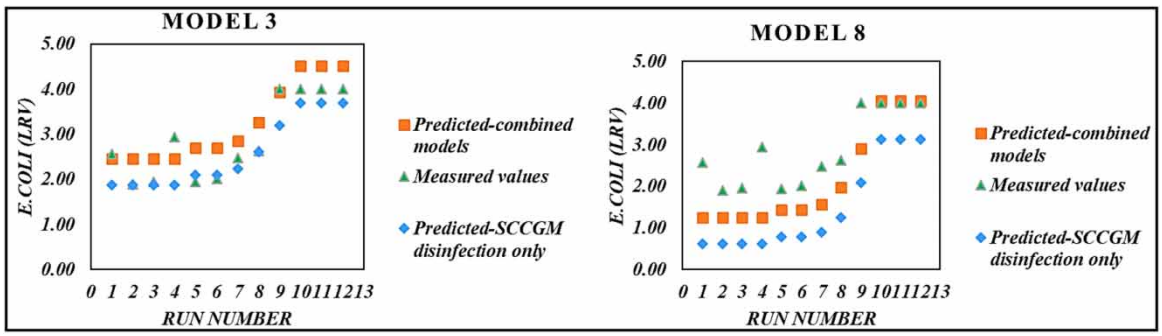

Figure 5 | Effect of modelling *E. coli* removal by disinfection only.

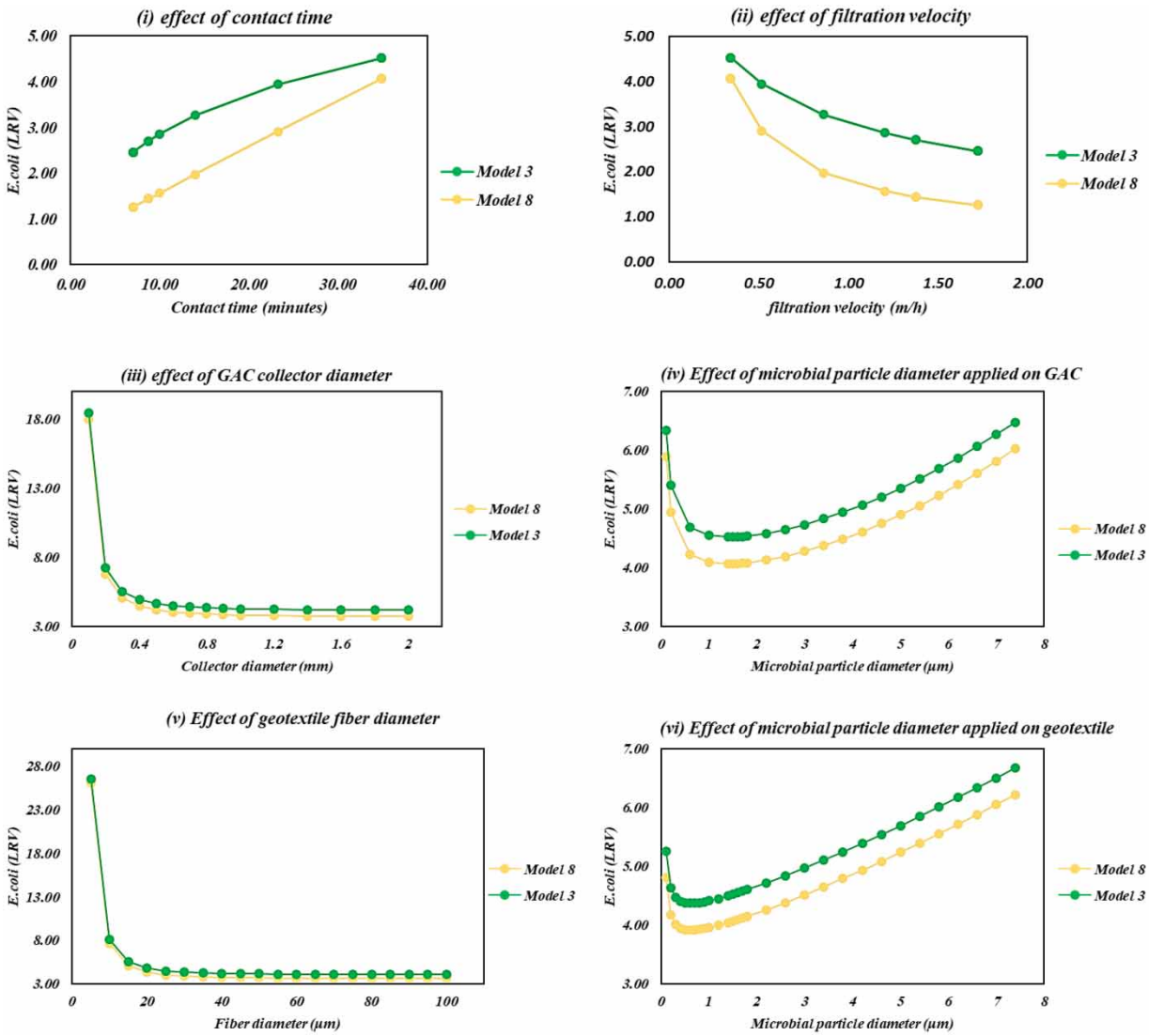

Figure 6 | Effect of contact time, filtration rate, collector diameter and microbial particle (*E. coli*) size.

Downloaded from http://iwaponline.com/ws/article-pdf/20/5/1757/728513/ws020051757.pdf
by STELLENBOSCH UNIVERSITY user

Table 5 | Model performance assessment for measured vs. predicted values

Mathematical model	R^2	RMSE	NOF	PBIAS
Model 1	0.822	0.887	0.309	25.4
Model 2	0.828	1.717	0.599	56.3
Model 3	0.826	0.520	0.181	−12.9
Model 4	0.820	0.885	0.309	25.3
Model 5	0.821	0.839	0.293	22.8
Model 6	0.825	1.639	0.572	53.7
Model 7	0.825	0.580	0.202	−15.5
Model 8	0.821	0.839	0.293	22.8

disinfection mechanisms by the multi-barrier system relatively well.

The silver disinfection component by these models was theoretically within the findings by Singh *et al.* 2019, who indicated that about 24 mg·min/L of Ct (silver concentration multiplied by time) value is required to eliminate 99% of *E. coli* from natural stream waters. The calculated Ct values in this study, which corresponded to approximately 99% (≈2 LRV) and higher, were >20 mg·min/L. These were from runs 8 to 12 (Table 4 and Figure 4). Further improvement of the models, particularly in terms of the input parameter values obtained or calculated from literature, could conceivably minimize the underestimations (by models 1, 4, 5 and 8) and overestimation (by models 3 and 7) of *E. coli* removals. Long term experimentation is therefore recommended to improve or calibrate the model input parameter values (especially those obtained from literature).

Models 3 and 7 may prompt the design engineer to under design the system, since the expected removals were higher than those measured. Conversely, models 1, 4, 5 and 8 may prompt the design engineer to over design the system. This shows that different model and removal mechanism combinations can produce different bacterial removal predictions. Therefore, using an array of models coupled with larger experimental data sets may help minimize under and over predictions and correspondingly minimize over and under designs of multi-barrier PoU water treatment systems such as the modelled system.

The higher removals by models 3 and 7 could be attributed to the silver disinfection by the Collins-Selleck model, which generally gave higher predictions for *E. coli* inactivation rates. On the other hand, silver disinfection by models 1 and 5 was simulated by the Chick's model while silver disinfection by models 4 and 8 was simulated by the Chick-Watson model. The Chick's and Chick-Watson models generally under predicted the *E. coli* inactivation rate. However, with further refinement, models 1, 4, 5 and 8 are tentatively expected to give a better match since their removals showed a more realistic gradual increment in *E. coli* removals, which closely corresponded to the contact time, as is theoretically supposed to be the case.

Figure 4 shows that models 2 and 6 were essentially unable to predict the *E. coli* removals. The weak predictions of the two models could be attributed to the CMS model (Equation (9)) being weak at simulating *E. coli* inactivation by silver in the SCCGM, which is the main disinfection step in the multi-barrier system. The CMS model predicts microbial inactivation by using natural die-off kinetics assuming microbial die-off with time (de Moel *et al.* 2007; Qasim & Zhu 2018). It may thus need higher contact time for substantial removals, and is principally applicable to bacterial die-off in non-disinfection treatment processes like natural treatment reservoirs (Qasim & Zhu 2018).

Effect of neglecting the filtration contribution by the SCCGM

The effect of neglecting filtration contribution by the SCCGM was assessed by essentially comparing the predicted removals by models 1–4 with the corresponding removals by models 5–8 (Figure 4). Modelling the additional removal contribution by SCCGM had minimal effect on the predicted overall removal (Figure 4 and Tables 4 and 5). This was not surprising because, except for advanced technologies such as reverse osmosis and iodine resin filters (Backer 2000), bacterial removal by fabric and granular filtration alone is primarily most efficient for suspended solids removal, not for removal of bacteria, due to large pore sizes (Backer 2002, 2000; Kausley *et al.* 2018; Siwila & Brink 2018). Therefore, fabric and granular filtration are normally used as a first stage before other treatment steps (Kausley *et al.* 2018). The need for an in-built disinfection step by silver in the SCCGM is therefore indicated. This finding is supported by literature from various authors where bacterial removal by silver-impregnated filter media (Chong *et al.* 2011; Rossainz-Castro *et al.* 2016; Shimabuku

Downloaded from http://iwaponline.com/ws/article-pdf/20/5/1757/728513/ws020051757.pdf
by STELLENBOSCH UNIVERSITY user

et al. 2018) was satisfactorily modelled by considering silver disinfection only without consideration of physical removal by filtration. Thus, porous media impregnated with silver or other metal disinfectants have been shown to be efficient at bacterial inactivation (Chong *et al.* 2011; Rossainz-Castro *et al.* 2016). However, disinfection may also be improved if fabric pre-filtration is provided to increase bacterial contact with the metal disinfectant (Tobiason *et al.* 2011) while GAC post filtration was provided to make the water more acceptable (Backer 2002; Tobiason *et al.* 2011).

Effect of modelling *E. coli* removal by disinfection only

It was assessed whether *E. coli* removal could be modelled by disinfection kinetics only (Figure 5) using two models (models 3 and 8) representing possible overestimation and underestimation. Thus, the removal of the coupled models was contrasted with removal by SCCGM disinfection alone. Model 3 was selected for this purpose over model 7 because it showed better performance statistics than model 7 (Table 5). Similarly, model 8 was chosen over models 1, 2, 4, 5 and 6 since it also depicted better statistics (Table 5). It can be seen from Figure 5 that, although *E. coli* removal prediction by SCCGM alone seemed to be a good representation, modelling additional removal by other treatment steps (i.e. geotextile and GAC removals) was still important for the models to be fully representative of the multi-barrier system. Thus, from the results shown in Figure 5, it can be seen that disinfection removal alone could not fully describe the *E. coli* removals, giving predicted LRVs below measured values for both models.

Effect of contact time, filtration rate, collector diameter and microbial particle *(E. coli)* size

The effect of contact time, filtration rate, collector diameter and microbial particle size on *E. coli* removal was assessed using models 3 and 8 (Figure 6). Both models indicated that larger contact time (Figure 6(i)) resulted in higher *E. coli* removal. Since contact time is dependent on filter media depth and filtration rate (see Equation (4)), optimizing either or both of the parameters optimizes contact time and subsequently enhances *E. coli* removals. Each of the models used in this study was affected by contact time and hence by media depth (h) and filtration rate (v). For instance, as filtration rate increases (Figure 6(ii)), *E. coli* removal by both models decreases. Therefore, careful optimization of these parameters is expected to enhance *E. coli* removal performance. It is worth noting that filtration rate is affected by various factors, of which particle size distribution is the key factor (Siwila & Brink 2020). Therefore, to optimise contact time it is necessary to not only look at filtration rate but also at factors affecting it, such as particle size distribution. If fine granules are insufficient in a filter media the filtration rate is very high, leading to lower contact time, while if coarse granules are insufficient the filtration rate is too low, leading to higher contact time. The collector diameter (d_c) depends on particle size distribution and subsequently affects *E. coli* removal prediction.

The sensitivity of models 3 and 8 to collector and fiber diameter is shown in Figure 6(iii) and 6(v). The smaller the collector or fiber diameter, the higher the removals (Figure 6(iii) and 6(v)). The sensitivity of microbial particle (*E. coli*) size was also assessed (Figure 6(iv) and 6(vi)). The effect of the collector/fiber diameter and microbial particle diameter were assessed by applying the varied particle sizes on the geotextile and GAC CFT models, which are directly affected by particle size. This analysis was done using the input parameters listed in Table 1 but keeping the optimal flow rate (2 L/h) constant. It can be seen from Figure 6(iv) and 6(vi) that the microbial particle diameter having the least removal efficiency by GAC and geotextile in both models is somewhere between 1 and 2 μm. Removal of microbial particles below this range increases with decreasing particle diameter because removal is primarily by diffusion (Yao *et al.* 1971; Tufenkji & Elimelech 2004), while removal of bacteria with diameters larger than 2 μm increases with particle diameter and removal is mainly by sedimentation and interception (Yao *et al.* 1971; Tufenkji & Elimelech 2004). This explanation consequently entails that removal of microbial particles by porous media filtration alone is a huge challenge. This finding is important because it further supports the need for a carefully optimized inbuilt disinfection step to ensure continued safety of the produced water. Overall, the sensitivity analysis results of predicted *E. coli* removals by models 3 and 8

Downloaded from http://iwaponline.com/ws/article-pdf/20/5/1757/728513/ws020051757.pdf
by STELLENBOSCH UNIVERSITY user

were significantly similar for each parameter assessed (Figure 6).

CONCLUSIONS AND RECOMMENDATIONS

The modelling exercise has demonstrated that suitable removal mechanisms can be integrally used to model a combined PoU system to predict the overall effluent bacterial quality. This kind of modelling can be used to optimize system design by allowing the engineer to systematically vary design parameters until the desired system effectiveness is attained. This research has also indicated that each barrier or treatment stage contributes to the overall *E. coli* removal. Therefore, the bacterial load on the SCCGM (which is the main disinfection stage) can be significantly reduced by optimizing all components of the multi-barrier (combined) system, especially the pre-filtration stage. Some reasons for differences between predicted *E. coli* inactivation and actual inactivation by models such as the Chick's and Chick-Watson models include (Qasim & Zhu 2018): (i) disinfectant residue may not be constant or uniform throughout the system and filter runs, (ii) pH changes may affect the inactivation rate, (iii) variations in the incoming suspended particle loads of the water being treated, (iv) varying temperature, and (v) the disinfectant may be consumed by other competitive reactions.

It is recommended that future research should keep the obtained optimal flow constant then model the breakthrough of *E. coli* for several runs, ensuring water is passed in triplicate for each run. Furthermore, modelling of data obtained from field testing to assess possible applicability of the mathematical models on field data is proposed. Also, concurrent modelling of *E. coli* and turbidity is proposed, since performance of filter systems is usually monitored by measuring effluent turbidity (MWH 2012). Additionally, since the proposed multi-barrier water treatment design is scalable such that the capacity is flexible and can be increased to serve more consumers, modelling the effect of scalability is proposed. Long term experimentation is also recommended, and may help in calibrating model parameters to achieve the best fit between the modelled and measured values. Quantification of measured influent and effluent *E. coli* counts using particle counting techniques is also recommended. This may help characterize the modelled microbial particle diameter (d_p) better.

REFERENCES

Backer, H. 2000 In search of the perfect water treatment method. *Wilderness and Environmental Medicine* **11**, 1–4.

Backer, H. 2002 Water disinfection for international and wilderness travelers. *Clinical Infectious Diseases Travel Medicine* **34**, 355–364. doi:10.1086/324747.

Bouwer, E. J. & Rittmann, B. E. 1992 Correspondence. Comment on 'Use of colloid filtration theory in modelling movement of bacteria through a contaminated sandy aquifer'. *Environmental Science & Technology* **26**, 400–401. doi:10.1021/es00026a025.

Brandt, M. J., Johnson, K. M., Elphinston, A. J. & Ratnayaka, D. D. 2017 *Twort's Water Supply*, 7th edn. Butterworth-Heinemann, Oxford, UK.

Brownell, S. A., Chakrabarti, A. R., Kaser, F. M., Connelly, L. G., Peletz, R. L., Reygadas, F., Lang, M. J., Kammen, D. M. & Nelson, K. L. 2008 Assessment of a low-cost, point-of-use, ultraviolet water disinfection technology. *Water Health* **6** (1), 53–65. doi:10.2166/wh.2007.015.

Center for Affordable Water and Sanitation (CAWST) 2011 *Introduction to Household Water Treatment and Safe Storage Training Participant Manual No. 01*. Managing Water in the Home, Calgary, Alberta, Canada.

Center for Affordable Water and Sanitation (CAWST) 2017 *Introduction to Drinking Water Quality for Household Water Treatment Implementers*. Technical Brief, Calgary, Alberta, Canada.

Chen, W. B. & Liu, W. C. 2015 Water quality modelling in reservoirs using multivariate linear regression and two neural network models. *Advances in Artificial Neural Systems* 521721. doi:10.1155/2015/521721.

Chick, H. 1908 An investigation of the laws of disinfection. *Hygiene* **8** (1), 92–158. doi:10.1017/S0022172400006987.

Chong, M. N., Jin, B. & Saint, C. P. 2011 Bacterial inactivation kinetics of a photo-disinfection system using novel titania-impregnated kaolinite photocatalyst. *Chemical and Engineering* **171** (1), 16–23. doi:10.1016/j.cej.2011.03.024.

Choo, C. & Tien, C. 1991 Hydrosol deposition in fibrous beds. *Separations Technology* **1** (3), 122–131. doi:10.1016/0956-9618(91)80007-M.

de Moel, P. J., Verberk, J. Q. J. C. & van Dijk, J. C. 2007 *Drinking Water: Principles and Practices*, Reprinted edn. World Scientific, New Jersey, USA.

Fulazzaky, M. A., Sunar, N. M., Abd Latiff, A. A. & Mohd Kassim, A. H. 2009 Empirical models of bio-sand filter to calculate the design parameters. *Water Science and Technology: Water Supply* **9** (6), 723–734. doi:10.2166/ws.2009.228.

Gikas, D. G. & Tsihrintzis, V. A. 2012 A small-size vertical flow constructed wetland for on-site treatment of household

Downloaded from http://iwaponline.com/ws/article-pdf/20/5/1757/728513/ws020051757.pdf
by STELLENBOSCH UNIVERSITY user

wastewater. *Ecological Engineering* **44**, 337–343. doi:10.1016/j.ecoleng.2012.04.016.

Guzy, C. J., Bonano, E. J. & Davis, E. J. 1983 The analysis of flow and colloidal particle retention in fibrous porous media. *Colloid Interface Science* **95** (2), 523–543. doi:10.1016/0021-9797(83)90212-6.

Hijnen, W. A. M., Suylen, G. M. H., Bahlman, J. A., Brouwer-Hanzens, A. & Medema, G. J. 2010 GAC adsorption filters as barriers for viruses, bacteria and protozoan (oo)cysts in water treatment. *Water Research* **44**, 1224–1234. doi:10.1016/j.watres.2009.10.011.

Horan, N. J. 2003 Fecal indicator organisms. In: *Handbook of Water and Wastewater Microbiology*. Elsevier, Amsterdam, The Netherlands, pp. 105–112. doi:10.1016/B978-012470100-7/50008-X.

Jenkins, M. W., Tiwari, S. K. & Darby, J. 2011 Bacterial, viral and turbidity removal by intermittent slow sand filtration for household use in developing countries: experimental investigation and modelling. *Water Research* **45** (18), 6227–6239. doi:10.1016/j.watres.2011.09.022.

Kausley, S. B., Dastane, G. G., Kumar, J. K., Desai, K. S., Doltade, S. B. & Pandit, A. B. 2018 *Clean Water for Developing Countries: Feasibility of Different Treatment Solutions, Encyclopedia of Environmental Health*, 2nd edn. Elsevier, Amsterdam, The Netherlands. doi:10.1016/B978-0-12-409548-9.11079-6.

Kaytech Engineering 2018 *Bidim General Civil Engineering Applications*. Available from: https://kaytech.co.za/ (accessed 20 February 2018).

Krause, P., Boyle, D. P. & Bäse, F. 2005 Comparison of different efficiency criteria for hydrological model assessment. European Geosciences Union. *Advances in Geosciences* **5**, 89–97. doi:10.5194/adgeo-5-89-2005.

Lantagne, D. & Yates, T. 2018 Household water treatment and cholera control. *The Journal of Infectious Diseases* JID 2018 **218**, S147–S153. doi:10.1093/infdis/jiy488.

Lee, Y. & Nam, S. 2002 Reflection on kinetic models to the chlorine disinfection for drinking water production. The microbiological society of Korea. *The Journal of Microbiology* **40** (2), 119–124.

Masters, G. M. & Ela, W. P. 2014 *Introduction to Environmental Engineering and Science*, 3rd edn, Pearson new international edition. Pearson, Harlow, UK.

Medema, G. J., Schets, F. M., Teunis, P. F. M. & Havelaar, A. H. 1998 Sedimentation of free and attached cryptosporidium oocysts and giardia cysts in water. *Applied & Enviromental Microbiology* **64** (11), 4460–4466.

Metcalf & Eddy 2014 *Wastewater Engineering: Treatment and Resource Recovery*, 5th edn, International edition. McGraw-Hill Education, New York, NY, USA.

MWH 2012 *MWH's Water Treatment: Principles and Design*, 3rd edn. MWH Global, Inc. John Wiley & Sons, Hoboken, NJ, USA.

Pandit, A. B. & Kumar, J. K. 2019 *Drinking water treatment for developing countries: physical, chemical and biological pollutants*. Royal Society of Chemistry, Cambridge, UK doi:10.1039/9781788012935-00021.

Qasim, S. R. & Zhu, G. 2018 *Wastewater Treatment and Reuse Theory and Design Examples, Volume 2: Post-Treatment, Reuse, and Disposal*. Taylor & Francis Group, Boca Raton, FL, USA.

Rajagopalan, R. & Tien, C. 1976 Trajectory analysis of deep-bed filtration with the sphere-in-cell porous media model. *American Institute of Chemical Engineers (Aiche) Journal* **22** (3), 523–533. doi:10.1002/aic.690220316.

Rietveld, L. 2019 *Drinking Water Treatment: Disinfection*. Delft University of Technology, Delft, The Netherlands. Available from: https://delftxdownloads.tudelft.nl/CTB3365DWx-DrinkingWaterTreatment/Module5/CTB3365DWx_2016_511_Disinfection-slides.pdf (accessed 15 March 2019).

Rijnaarts, H. H. M., Norde, W., Bouwer, E. J., Lyklema, J. & Zehnder, A. J. B. 1995 Reversibility and mechanism of bacterial adhesion. *Colloids and Surfaces B: Biointerfaces* **4** (1), 5–22. doi:10.1016/0927-7765(94)01146-V.

Rossainz-Castro, L. G., De-La-Rosa-Gómez, I., Olguín, M. T. & Alcántara-Díaz, D. 2016 Comparison between silver- and copper-modified zeolite-rich tuffs as microbicide agents for *Escherichia coli* and *Candida albicans*. *Environmental Management* **183**, 763–770. doi:10.1016/j.jenvman.2016.09.034.

RWSN (Rural Water Supply Network) 2010 Myths of the Rural Water Supply Sector. Rural Water Supply Network (RWSN) Perspectives No. 4, Paper prepared by the RWSN Executive Steering Committee.

Shimabuku, Q. L., Ueda-Nakamura, T., Bergamasco, R. & Fagundes-Klen, M. R. 2018 Chick-Watson kinetics of virus inactivation with granular activated carbon modified with silver nanoparticles and/or copper oxide. *Process Safety and Environmental Protection* **117**, 33–42. doi:10.1016/j.psep.2018.04.005.

Singh, R., Edokpayi, J. N., Odiyo, J. O. & Smith, J. A. 2019 *E. coli* inactivation by metals and effects of changes in water chemistry. *Environmental Engineering* **145**, 04018136. doi:10.1061/(ASCE)EE.1943-7870.0001486.

Siwila, S. & Brink, I. C. 2018 Low cost drinking water treatment using nonwoven engineered and woven cloth fabrics. *Water Health* **17** (1), 98–112. doi:10.2166/wh.2018.226.

Siwila, S. & Brink, I. C. 2020 A novel low-cost multi-barrier system for drinking water treatment in rural and suburban areas. *Water Practice and Technology* **15** (1), 48–65. doi:10.2166/wpt.2019.083. Available from: https://iwaponline.com/wpt/article/15/1/48/71649/A-novel-lowcost-multibarrier-system-for-drinking.

Somani, S. & Ingole, N. 2012 Formulation of kinetic model to predict disinfection of water by using natural herbs. *International Journal of Environmental Sciences* **2** (3), 1344–1354. doi:10.6088/ijes.0020203002.

TAM Ceramics 2019 *About TAM Ceramics*. Available from: https://tzenvirohealth.wixsite.com/aboutus (accessed 11 January 2019).

Downloaded from http://iwaponline.com/ws/article-pdf/20/5/1757/728513/ws020051757.pdf
by STELLENBOSCH UNIVERSITY user

Tien, C. 2012 *Principles of Filtration*, 1st edn. Elsevier, Amsterdam, The Netherlands. doi:10.1016/B978-0-444-56366-8.00001-3.

Tobiason, J. E., Cleasby, J. L., Logsdon, G. S. & O'Melia, C. R. 2011 *Granular Media Filtration in Water Quality & Treatment: A Handbook on Drinking Water*. American Water Works Association, Denver, CO, USA.

Treacy, J. 2019 Drinking water treatment and challenges in developing countries. In: *The relevance of hygiene to health in developing countries*. IntechOpen, London, UK. doi:10.5772/intechopen.80780.

Tufenkji, N. & Elimelech, M. 2004 Correlation equation for predicting single-collector efficiency in physicochemical filtration in saturated porous media. *Environmental Science & Technology* **38** (2), 529–536. doi:10.1021/es034049r.

Tufenkji, N., Redman, J. A. & Elimelech, M. 2003 Interpreting deposition patterns of microbial particles in laboratory-scale column experiments. *Environmental Science & Technology* **37** (3), 616–623. doi:10.1021/es025871i.

Wakeman, R. J. & Tarleton, E. S. 2005 *Solid/Liquid Separation: Principles of Industrial Filtration*, 1st edn. Elsevier Advanced Technology, Oxford, UK.

WHO 2017 *Water Quality and Health-Review of Turbidity: Information for Regulators and Water Suppliers*. Available from: http://apps.who.int/iris/bitstream/10665/254631/1/WHO-FWC-WSH-17.01-eng.pdf (accessed 30 March 2019).

Yao, K. M., Habibian, M. T. & O'Melia, C. R. 1971 Water and wastewater filtration. Concepts and applications. *Environmental Science & Technology* **5** (11), 1105–1112. doi:10.1021/es60058a005.

First received 20 November 2019; accepted in revised form 21 April 2020. Available online 7 May 2020

Downloaded from http://iwaponline.com/ws/article-pdf/20/5/1757/728513/ws020051757.pdf
by STELLENBOSCH UNIVERSITY user